

Evolving Starburst Modeling of FIR/sub-mm/mm Line Emission.

III. Application to Nearby Luminous Infrared Galaxies

Lihong Yao

*Department of Astronomy and Astrophysics, University of Toronto, Toronto, ON M5S
3H8, Canada*

yao@astro.utoronto.ca

ABSTRACT

We present a preliminary study of using the template of an ensemble of evolving shells we developed for M 82 (Yao 2009). we apply the model to represent various stages of starburst evolution in a well known sample of nearby luminous infrared galaxies (LIRGs). In this way, we attempt to interpret the relationship between the degree of molecular excitation and ratio of far-infrared (FIR) to ^{12}CO (or simply CO) luminosity to possibly reflect different stages of the evolution of star-forming activity within their nuclear regions.

Subject headings: ISM: clouds – ISM: evolution – galaxies: ISM – galaxies: starburst – galaxies: star clusters – radio lines: ISM

1. Introduction

Knowledge of the properties and evolution of molecular gas and dust content in the interstellar medium (ISM) of starburst galaxies is essential for understanding the cause and evolution of starburst activity. In particular, studies of such galaxies in the local universe are important in understanding the role of starburst phenomenon in the cosmic evolution of galaxies. To constrain theories of how the ISM evolves, one needs to investigate both individual galaxies and large statistical samples of data at multiple wavelengths. Especially, with the available data for the dust component, studying the gas in the co-space ISM becomes more interesting and important.

Starburst galaxies have impressive reservoirs of molecular gas in their centers to fuel the massive star formation. Bursts of massive star formation can dramatically alter the structure and evolution of their host galaxies by injecting large amounts of energy and mass into the ISM via strong stellar radiation, repeated supernova explosions, and cosmic rays. Hence, the

main excitation mechanisms for molecular gas in starburst regions are the combination of collisional process in dense gas and strong UV radiation field stemming from photoelectric heating, far-UV pumping of H₂, strong mechanical energy, enhanced cosmic rays and X-rays, as well as shock and turbulent heating.

The number of multiwavelength observations of starburst galaxies throughout the cosmic-scale has increased dramatically due to the significant improvement in the sensitivity and resolution of telescopes. These observations provide an essential basis for starburst modeling, and such modeling provides systematic predictions of the properties of the ISM in idealized models of starburst galaxies for comparison with these observations. In a previous paper (Yao 2009, hereafter Paper II), we presented an unique set of starburst models that allow us *first time* to relate observed molecular line properties of a starburst region to its age and provided better interpretations for the observations. In our model, the molecular gas responding to star formation in a starburst galaxy is treated as an ensemble of GMCs with different initial masses, each of which responds to massive star formation at its center. The four physics elements incorporated in our model are a standard similarity solution for the bubble/shell structure around a young star cluster, a time-dependent stellar population synthesis method, a fully time-dependent chemistry problem for the PDRs, and a non-LTE radiative transfer method for molecular and atomic lines (Yao et al. 2006; Yao 2009b). Detailed discussion of each of these individual elements and why they are important in evaluating the physical and chemical properties of molecular gas in a starburst galaxy, are presented in the Ph.D. thesis of Yao (2009a, and references therein, hereafter Yao Thesis).

In Papers I and II, we have successfully demonstrated that the kinematic and far-infrared/sub-millimeter/millimeter (FIR/sub-mm/mm) emission properties of individual expanding shells and star-forming regions in nearby prototypical starburst galaxy M 82 can be understood by following the evolution of individual massive super star clusters (Yao 2006, hereafter Paper I) or an ensemble of such clusters surrounded by compressed shells and GMCs (Paper II). We found that the spectral energy distributions (SEDs) of the molecular and atomic line emission from these swept-up shells and the associated parent giant molecular clouds (GMCs) contains a *signature* of the stage of evolution of the starburst. We suggested that the physical and chemical properties of molecular and atomic gas and their excitation conditions depend strongly on the stage of starburst evolution in the central kiloparsec region of M 82.

At distances beyond M 82, the submillimeter common user bolometer array (SCUBA) sources represent an distinct population from low- z to high- z universe. Multiwavelength studies of these galaxies at the local universe, for example, the SCUBA local universe galaxy (SLUGS) surveys (Dunne et al. 2000; Thomas et al. 2002; Yao et al. 2003), has revealed that

the properties of molecular gas and dust in the central starburst regions differ significantly from that of quiescent star forming disks and the center of our Galaxy. The SLUGS dust submillimeter survey contains 104 galaxies selected from *IRAS* bright galaxy sample, with a flux limit of $S_{60} > 5.24$ Jy, and FIR luminosities in the range $10^{10} L_{\odot} < L_{FIR} < 10^{12} L_{\odot}$, and the SLUGS CO survey contains about 60 SLUGS galaxies over a restricted range in RA. It is essentially complete to the same *IRAS* flux.

In § 2 of this paper we present the application of our evolving starburst models to the SLUGS sample, using the template of a shell ensemble we developed for M 82 (see Paper II). We examine one interesting and yet puzzling issue in particular - whether the relation between the degree of molecular gas excitation and the star formation properties in these SLUGS objects can be understood in terms of our evolving starburst model as a preliminary study. This issue is a follow-up to an earlier observational paper by Yao et al. (2003) in which a clear connection between these two properties was identified. We also investigate whether the variations in these properties from galaxy to galaxy may derive simply from seeing galaxies in different stages of their post starburst evolution, as seen in our models. Previous interpretation of these effects require that they reflect the diversity in the intrinsic properties of galaxies, with no necessary connection to starburst evolutionary phases.

Low-lying CO rotational line transition at millimeter wavelength (CO $J = 1 - 0$) is often used as a tracer of the total molecular hydrogen content in a galaxy (e.g. Mauersberger 1996; Mauersberger et al. 1999; Yao et al. 2003). But it is not a good tracer of dense or warm gas in star-forming regions. The most common method of deriving H₂ masses from ¹²CO(1-0) luminosities relies on a reliable estimate of the controversial parameter X , which converts CO line intensity or luminosity to the H₂ column density or mass. Previous studies have shown that this parameter varies from galaxy to galaxy (Booth & Aalto 1998; Boselli et al. 2002; Zhu et al. 2009), and it is thought to be higher in metal-poor galaxies and lower in starburst galaxies than in Galactic molecular clouds, where X is about $2.8 \times 10^{20} \text{ cm}^{-2} [\text{K km s}^{-1}]^{-1}$ (Bloemen et al. 1986; Strong et al. 1988). Hereafter we refer to this as the standard value. Thus in starburst galaxies, application of the standard factor can produce a significant overestimate (4 - 10 times) of molecular hydrogen mass (Solomon et al. 1997; Downes & Solomon 1998; Yao et al. 2003). The question we ask is:

Does the X-factor depend on the phase of starburst evolution?

In § 3 of this paper, as a separate issue, we present the *first attempt* of exploring the time dependence in our models of this well known controversial CO-to-H₂ conversion factor X in starburst regions.

Starbursts remain a viable explanation for the dominant energy source in luminous infrared galaxies at the local universe. An instantaneous starburst model is therefore assumed here for the studies of the SLUGS galaxies, the same as our previous studies of nearby starburst galaxy M 82 (Paper II). The instantaneous burst scenario may not be physically realistic for SLUGS galaxies, but it is an acceptable representation of the molecular CO line SED if the duration of the star-forming event in their centers is shorter than the starburst age (Yao 2009a). The set of our starburst models is divided into two phases (as defined in Paper II), the *Winds* phase comprises younger and denser shells than in the *post-SN* phase. These two phases are treated independently, and can be viewed as simply alternative scenarios.

2. Correlation between CO Excitation and Star Formation Properties

We first compute the relevant star formation related characteristics as a function of time for a model shell ensemble, then we compare these predicted characteristics with those observed in a modest but nearly complete sample of nearby luminous IR galaxies. Each galaxy in the sample is presumed to represent a different evolutionary stage of our model starburst. Ratios of quantities, specifically, $^{12}\text{CO}(3-2)$ to $(1-0)$ line intensity ratio r_{31} (Yao et al. 2003), and FIR luminosity to molecular gas mass ratio $L_{FIR} / M(\text{H}_2)$, are used in our analysis. These ratios describe intrinsic properties independent of galaxy size and assumed distance. In the standard literature, the L_{FIR} is used as an indicator of star formation rate (SFR) (Kennicutt 1998a), and the quantity L_{FIR} / L_{CO} or $L_{FIR} / M(\text{H}_2)$ is taken to be a measure of the star formation efficiency (SFE) (Yao et al. 2003), i.e. star formation rate per unit available gas mass. However, in our model this ratio does not measure star formation efficiency, but is a parameter which undergoes a dramatic evolution during the tens of millions of years following a starburst event. The far-infrared luminosity L_{FIR} ($10 < \lambda < 100 \mu\text{m}$) can be readily derived from a dusty starburst model, but not by our gas model. In this paper, we use the stellar cluster luminosity L_{SC} to represent the L_{FIR} , by crudely assuming that all of the stellar light is processed into far-infrared by dust enshrouding the star clusters and distributed in the galaxies. The ratio of $^{12}\text{CO}(3-2)$ to $(1-0)$ line emission r_{31} is known to provide a more sensitive measure of the gas temperature and density than the ratio of $^{12}\text{CO}(2-1)$ to $(1-0)$ lines (e.g. Mauersberger et al. 1999). The r_{31} ratio is often used to measure the degree of molecular CO excitation.

An important feature observed in luminous IR galaxies is that the degree of ^{12}CO excitation has a trend of increasing with increasing concentration and efficiency of star-forming activity (Yao et al. 2003). Here we examine the effects of starburst phase in our model on the excitation ratio r_{31} by comparing a theoretical plot based on our results of

Chapter 4 with this observed relationship found in Yao et al. (2003) (see Fig. 1). We begin with the explanation of the effect outlined by Yao et al. (2003), and follow this with a different possible origin based on our starburst evolution scenario.

Fig. 1 (see also Fig. 10 of Yao et al. (2003)) shows that there is a significant observed correlation between r_{31} and $L_{FIR}/M(\text{H}_2)$ within the $15''$ aperture for the data with $L_{FIR}/M(\text{H}_2) \leq 200 L_\odot/M_\odot$. The SLUGS sample shown is divided into two ranges by gas mass centered at $M(\text{H}_2) = 10^8 M_\odot$, and also by dust FIR luminosity centered at $L_{FIR} = 10^{10} L_\odot$ which are indicated by three different symbols in the plot. The segmentation according to gas mass-range and dust IR luminosity-range shows the relationship between L_{FIR} and $M(\text{H}_2)$ and position in the plot. The linear correlation coefficient is 0.74 at a significance level of 1.4×10^{-7} (i.e. probability that r_{31} and SFE are related is significant). However, the correlation is diminished at $L_{FIR}/M(\text{H}_2) > 200 L_\odot/M_\odot$, where r_{31} ranges between 0.5 and 1.72 (Yao et al. 2003). The molecular gas mass in the SLUGS sample is derived from CO luminosities by applying the conversion factor $X = 2.7 \times 10^{19} \text{ cm}^{-2} [\text{K km s}^{-1}]^{-1}$ estimated using an large velocity gradient (LVG) analysis (Yao et al. 2003), which is about 4-10 times lower than the conventional X value derived from the Galaxy (Kenney & Young 1989). Hence, the result is $M(\text{H}_2) = 1.1 \times 10^3 D_L^2/(1+z) S_{CO} M_\odot$, where D_L is the luminosity distance of a galaxy in Mpc, and S_{CO} is the $^{12}\text{CO}(1-0)$ flux in Jy km s^{-1} measured within a $15''$ beam. According to Yao et al. (2003), both r_{31} and $L_{FIR}/M(\text{H}_2)$ ratios are found to be independent of the galaxy distance (or the projected beam size on galaxy), and in turn the H_2 gas mass. There are also no significant correlations found between r_{31} and star formation rate (or L_{FIR}), dust temperature and mass, the color indices, or the luminosity of the IR or radio continuum. Yao et al. suggested that the observed correlation between r_{31} and $L_{FIR}/M(\text{H}_2)$ and the lack of correlation of r_{31} with properties related to total star formation implies a dependence only on localized conditions within the molecular clouds. According to this picture, the dependence of r_{31} on the $L_{FIR}/M(\text{H}_2)$ ratio reflects a higher degree of CO excitation that is associated with a higher spatial concentration and efficiency of star forming activity. Such conditions would arise in an intense starburst where the surface density of such activity is high. The saturation effect (approaching unity) of r_{31} seen at $L_{FIR}/M(\text{H}_2) > 200 L_\odot/M_\odot$ reflects a limit imposed on this ratio at the highest excitation where the excitation temperatures for $^{12}\text{CO}(3-2)$ and $(1-0)$ (both assumed optically thick) are equivalent.

As mentioned earlier the $L_{FIR}/M(\text{H}_2)$ ratio is traditionally used as an indicator of star formation efficiency. In our model, this ratio and its variation with time are simple and direct consequences of the evolution in stellar luminosity (represented by L_{SC}) and swept-up gas mass within a single starburst. Fig. 1 also shows the model r_{31} ratio versus the $L_{SC}/M(\text{H}_2)$ ratio, where the total cluster luminosity L_{SC} has been used in place of the observed FIR

luminosity L_{FIR} . This assumes that the FIR luminosity produced in a recent starburst is the dominant component of the FIR luminosity. The $M(\text{H}_2)$ for the model is derived from S_{CO} , thus using the same method as employed for the SLUGS sample except with a fixed $D_L = 3.25$ Mpc used in our model computations. Thus, S_{CO} and $M(\text{H}_2)$ are both functions of time and size of the shells. The model curve clearly shows a trend similar to that in the observation, that is the r_{31} ratio increases with increasing $L_{SC}/M(\text{H}_2)$ ratio, and then saturates at high $L_{SC}/M(\text{H}_2)$ ($> 200 L_\odot/M_\odot$). The model r_{31} ratios vary between 0.7 and 1.3 for the *Winds* phase, and between 0.4 and > 2.0 for the *post-SN* phase. The key point associated with our model results shown in Fig. 1 is that the relationship between r_{31} and L_{SC} is governed by the age or phase of the starburst. At earlier stages the cluster luminosity is high and the mass of swept-up gas is small. Since the shells are comparatively small and expanding rapidly, they are also more effectively heated and compressed than at later stages. Thus, at earlier phases, both r_{31} and $L_{SC}/M(\text{H}_2)$ are higher than in the later phases of the expansion. Since the parent GMCs contribute more to the $^{12}\text{CO}(1-0)$ line than the (3-2) line, the r_{31} ratio is lower for the *Winds* phase, although the L_{SC} is higher than that from the *post-SN* phase. An important point associated with this interpretation is that the degree of molecular gas excitation is a consequence of star-forming activity, rather than a reflection of initial conditions prior to the starburst, as often assumed.

As described above, our model yields a result similar to the observations (i.e. possibly an upper limit of the observed data) and suggests that the observed behavior results from recent starbursts in these infrared luminous galaxies. This result furthermore implies that the relationship between the degree of CO excitation (r_{31}) and the $L_{FIR}/M(\text{H}_2)$ ratio associated with star formation properties may be determined by the phase of the starburst rather than by the more traditional view of variation in the efficiency of star formation.

One of the interesting properties of Fig. 1 is that the observed data points tend to concentrate toward the origin. A similar effect is discernible in the theoretical plot if points are plotted at equal intervals in age. The concentration in the latter case occurs because the rate of change of the variables on both axes decreases with time as the age becomes large. This suggests a further test of the hypothesis that the observed behavior in Fig. 1 is the consequence of seeing starbursts in different stages of their evolution. Accordingly, we compare the frequency distribution (or histogram) of the 45 SLUGS galaxies with respect to the observed $L_{FIR}/M(\text{H}_2)$ and r_{31} ratios to the frequency distribution of 45 pseudo galaxies with respect to the model $L_{SC}/M(\text{H}_2)$ and r_{31} ratios, as shown in Figs. 2 and 3. The pseudo galaxies were assigned ages drawn randomly from a uniform probability distribution between 3 Myr and 20 Myr, and the parameters r_{31} and $L_{SC}/M(\text{H}_2)$ then computed for these ages using our model. The model age range (3 - 20 Myr) reflects the range of validity of the model for the *post-SN* phase. The lower boundary corresponds to a plausible lower limit on

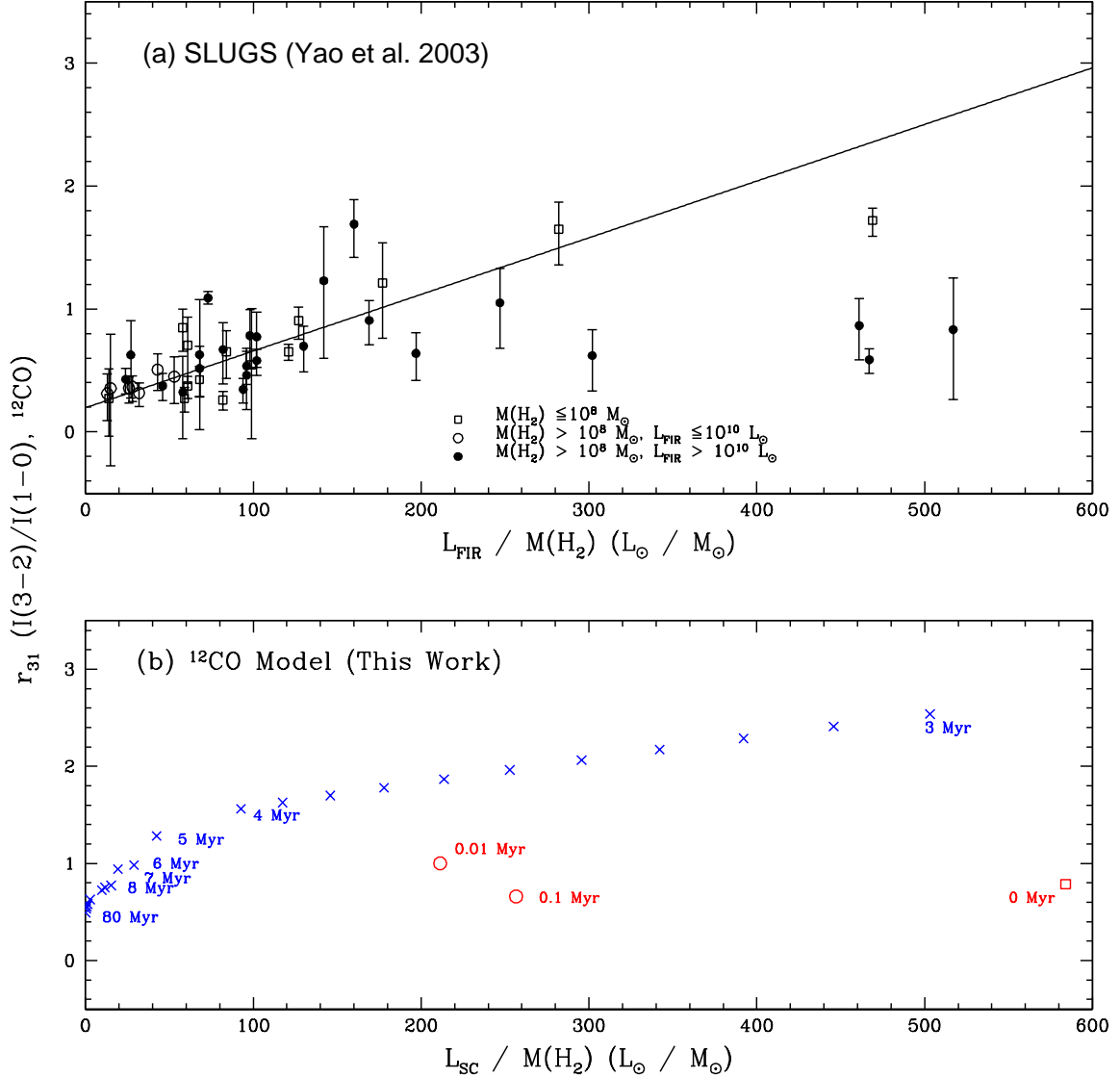


Fig. 1.— Plots of the line intensity ratio r_{31} (expressed as brightness temperatures integrated over velocity) versus the $L_{\text{FIR}}/M(\text{H}_2)$ ratio. Plot (a) is the observed r_{31} versus the $L_{\text{FIR}}/M(\text{H}_2)$ measured within a $15''$ aperture for the SLUGS sample. The line represents a linear regression fit to the data with $SFE \leq 200 L_{\odot}/M_{\odot}$. Plot (b) is our model result. Red open symbols (square: $t < 0.01$ Myr, circle: $0.01 \leq t \leq 0.1$ Myr, triangle: $0.1 - 0.7$ Myr) are for the *Winds* phase, and blue crosses are for the *post-SN* phase. The age sequence for the *post-SN* from right to left is 3, 4, 5, ..., 80 Myr.

the dynamical timescale for the starburst region and the upper boundary corresponds to the epoch beyond which the bubble shells escape the disk of the galaxy. The comparison reveals a similarity in the distributions between model and observation for both $\log_{10} (L_{FIR}/M(\text{H}_2))$ and r_{31} , though the peak in the former distribution occurs at a lower value in the model (see later for further discussion of this point). The qualitative similarity between the two histograms thus supports the hypothesis that the quantities $L_{FIR}/M(\text{H}_2)$ and r_{31} are related to starburst age. However, the evidence presented is not conclusive, merely suggestive.

We also tested our model result with different starburst age ranges (1 to 10 Myr and 1 to 80 Myr) for the 45 pseudo galaxies. These tests produced numerically different but qualitatively similar results.

As noted, the foregoing analysis supports the hypothesis that the plots in Fig. 1 signify that the excitation of the gas following a starburst is closely related to the age of the starburst. However, there are a number of considerations which need to be examined which may affect the credibility of this result, for example, the selection effect on the observed frequency distributions. Fortunately, the SLUGS subsample investigated here is nearly complete with a limiting FIR flux density and a limiting distance, so that the selection effects are well understood. Essentially all members of the sample are detected at both CO transitions, but the flux limit imposes a minimum detectable luminosity which increases with D_L^2 . The dramatic decline in galaxy number density with distance confirms this selection and indicates that the sample comprises the high luminosity tail of the underlying galaxy population. The question then is: could the luminosity selection affect the distribution of $L_{FIR}/M(\text{H}_2)$, particularly in producing a deficiency of ratios below the peak of the observed distribution? There are two approaches to investigate this effect. First, we can examine the direct relations between $L_{FIR}/M(\text{H}_2)$ and galaxy distance, as well as r_{31} and galaxy distance. We find no significant correlation between these two quantities and distance. Second, we divide the sample of 45 SLUGS galaxies into two parts, each with 23 objects, divided according to $D_L < 45$ Mpc and $D_L \geq 45$ Mpc. We find no significant difference between the frequency distributions of $L_{FIR}/M(\text{H}_2)$ in these two subgroups. Thus, there is no evidence that the selection effect in luminosity produces a corresponding selection in the ratio $L_{FIR}/M(\text{H}_2)$. We also conducted a similar analysis for the ratio r_{31} , and there is also no evidence of selection effect on this ratio.

Other observational effects, for example, the random and systematic errors in the observed data, would contribute to the disagreement between the model and the observed histograms, assuming that the theory were the correct explanation for the observation. It must also be recalled here that there is a deficiency of about an order of magnitude between model and observation in the total stellar luminosity for M 82. This deficiency in the model

luminosity will contribute to, and possibly even account for, the systematic difference in location of the peak of the two distributions of $L_{FIR}/M(\text{H}_2)$ shown in Fig. 2.

The hypothesis presented here that the ratios r_{31} and $L_{FIR}/M(\text{H}_2)$ are related to the starburst age can be further tested by direct measurements of the ages of the young stellar populations in the SLUGS subsample. Probably the best approach would be the fitting of population synthesis models to optical and IR spectroscopy of SLUGS objects, as discussed in Chapter 5.

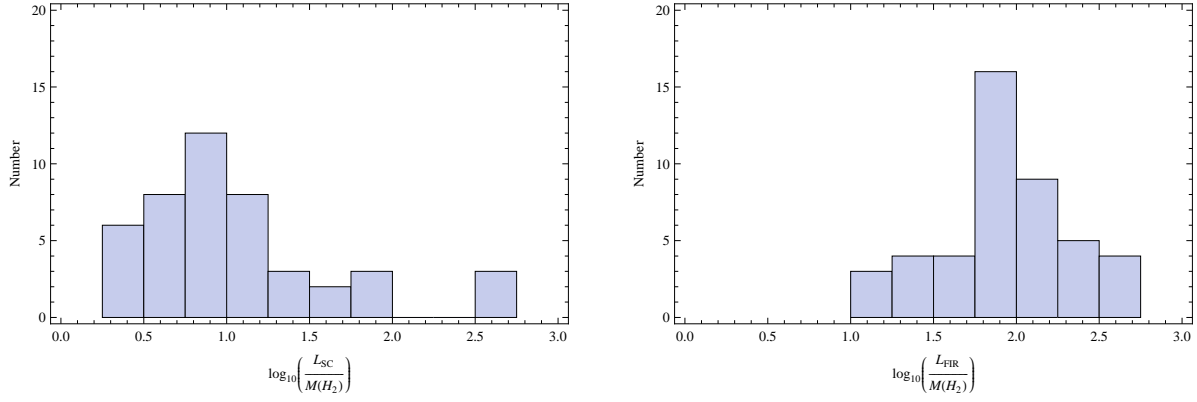


Fig. 2.— Histograms of the $L_{SC}/M(H_2)$ ratio derived from our starburst model and the $L_{FIR}/M(H_2)$ ratio measured for 45 SLUGS galaxies by Yao et al. (2003).

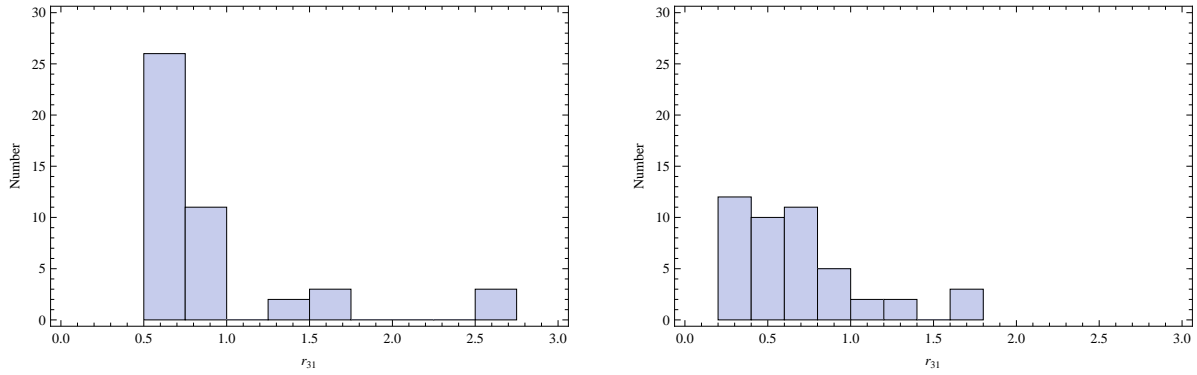


Fig. 3.— Histograms of the $^{12}\text{CO}(3-2)/(1-0)$ line ratio (r_{31}) derived from our starburst model and the r_{31} ratio measured for 45 SLUGS galaxies by Yao et al. (2003).

3. The CO-to-H₂ Conversion Factor X

Our evolving starburst model allows us to investigate, purely from a theoretical standpoint, the relationship between the X -factor and starburst phase, because the physical properties of molecular gas in an evolving starburst region changes with time. The X -factor may be determined from the following equation,

$$X(t) = \frac{M(H_2)}{4.1 \times 10^2 D_L^2 S_{CO}} \quad (1)$$

where $M(H_2)$ is the total H₂ gas mass swept up by the shells at time t in units of M_\odot , D_L is the luminosity distance, in this case to M 82 (used in our model computations) in unit of Mpc, S_{CO} is the ¹²CO(1-0) line flux in units of Jy km s⁻¹, and X value is in units of 10¹⁹ cm⁻² [K Km s⁻¹]⁻¹.

In the *Winds* phase, the value of X mainly increases with time. Because the parent GMCs are the dominant sources of ¹²CO(1-0) line emission during the earlier *Winds* phase, and because the gas inside the parent clouds is highly excited due to high FUV radiation, this results in a progressive decrease in ¹²CO(1-0) line emission from the GMCs with decreasing GMC mass. On the other hand, the compressed dense gas inside the shells is also highly excited, but the ¹²CO(1-0) line emission increases with increasing swept-up mass of the shells. Overall the ¹²CO(1-0) line emission from the shell and GMC ensemble increases with time, and slightly decreases from 0.5 to 0.7 Myr, while the system H₂ mass is fixed at $1.9 \times 10^7 M_\odot$. In the *post-SN* phase, the X -factor mainly increases with time, because the ¹²CO gas is highly excited at early stages of this phase. Although both the ¹²CO(1-0) line emission and swept-up shell mass $M(H_2)$ increase with time, the increasing rate in $M(H_2)$ is higher than that in the ¹²CO(1-0) luminosity between 5 and 80 Myr. However, the increasing rate in $M(H_2)$ is lower than that in the ¹²CO(1-0) luminosity in a brief interval between 2 and 5 Myr, producing a brief decline in the value of X shown in Fig. 4. The discontinuity between 0.8 and 1 Myr corresponds to the transition between *Winds* and *post-SN* phases.

The values for the X -factor derived from our models for the two best fit ages (5.6 and 10 Myr) for the central 1 kpc starburst regions of M 82 are 9.5×10^{19} and 1.1×10^{20} cm⁻² [K km s⁻¹]⁻¹, respectively. These values are comparable to the empirical values found from the studies of starburst galaxies (Weiss et al. 2001, Downes & Solomon 1998). They also lie between those derived for the Galaxy and nearby LIRGs (Yao et al. 2003). Our model X -factor shows a trend of increasing with time in the *post-SN* phase, i.e. lower values are associated with more highly excited gas. This is consistent with the observed results indicated in the above references, since starburst galaxies have lower values than those of

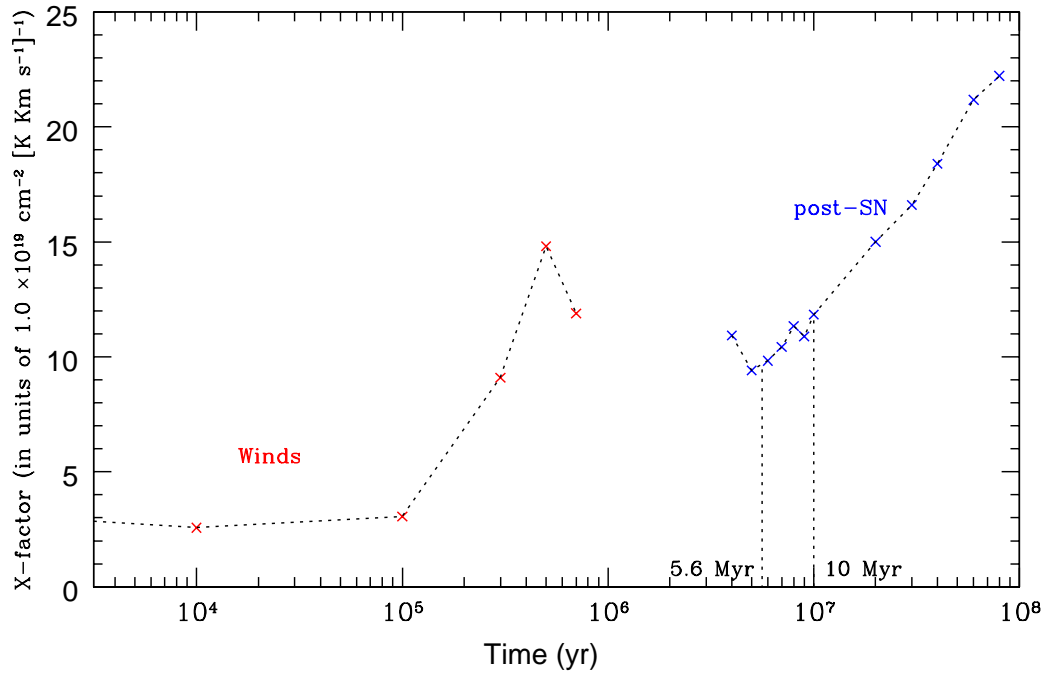


Fig. 4.— Plot of our model CO-to-H₂ conversion factor X as a function of time. Red cross symbols connected with black dashed curve are for the *Winds* phase, and blue crosses connected with black dashed curve are for the *post-SN* phase. The two best fitted ages (5.6 and 10 Myr) are also indicated in the plot.

the non-starburst (or normal) galaxies like our own Galaxy.

We also investigated the effect of reducing the upper mass limit on the GMC mass spectrum (i.e. from $10^7 M_\odot$ to $3 \times 10^6 M_\odot$ and $10^6 M_\odot$) on our model X -factor as was done for the ^{12}CO model in Chapter 5. Recall that in Chapter 5 we conclude that the model can provide acceptable fits to the data only if the dominant initiating starburst clusters are massive, at least $5 \times 10^5 M_\odot$. Here we find that the X value is also very sensitive to the assumed initial upper mass limit of the cluster spectrum (and corresponding GMC mass spectrum). For the first case with a slightly lower upper limit of GMC mass $3 \times 10^6 M_\odot$ (corresponding to stellar mass of $7.5 \times 10^5 M_\odot$), we found a solution similar to the result presented in Fig. 4. The value of X is about 15% and less for the *Winds* phase, but it is about a factor of 1.4 higher at 5.6 Myr and 1.2 higher at 10 Myr for the *post-SN* phase. But for the second case with a ten times or more reduction in the upper cutoff of the GMC (and cluster) mass spectrum, the value of X starts showing an opposite trend of decreasing with time, because in this case the increasing rate in $^{12}\text{CO}(1-0)$ luminosity is faster than the increasing rate in $M(\text{H}_2)$ mass swept up by the shells. The value of X is about 45% less for the *Winds* phase, but it is about a factor of 5 higher at 5.6 Myr and 2.3 higher at 10 Myr for the *post-SN* phase. Hence, acceptable solutions for modeling the X -factor in starburst galaxies are obtained only when our model system is dominated by initiating starburst clusters that are massive, at least $5 \times 10^5 M_\odot$.

The accuracy of the X -factor predicted by our model is limited by several conditions. The CO flux for a given H_2 mass depends upon a variety of factors which were discussed in Paper II (e.g. the dependence on the assumed turbulent velocity, the neglect of the CO emission from the ambient ISM). Equally important however is that the X -factor will depend to some degree on the assumed mass spectrum for the star clusters (as shown above), and on the assumed relation governing the expansion of the bubble driven shells. The latter relation governs the amount of H_2 mass swept up in a given period of time and the hence also the number of star clusters required to produce the total observable H_2 mass, as discussed also in Chapter 5.

It is important to understand that a precise value for the X -factor ultimately relies exclusively on the empirical determinations involving careful measurements of CO luminosity and H_2 mass. What our results do show, however, is that these empirical values may be reasonably replicated by a starburst model of the type investigated in this thesis, and that considerable insight regarding the causes of the variation from galaxy to galaxy may be obtained from the temporal behavior in our model exhibited during the expansion of the starburst bubbles/shells.

4. Conclusions

As a preliminary approach, we have shown that:

1. By comparing our starburst model to a limited extent with our published ^{12}CO observations of 45 nearby luminous IR galaxies, it yields some insight into the relevance of starburst evolution in a larger context. Both the model and the data show that the degree of CO excitation r_{31} increases with the increasing ratio $L_{FIR}/M(\text{H}_2)$, and that the frequency distributions of these two parameters in both the model prediction and the data are similar. This suggests that the observed behavior possibly results from recent starbursts in these galaxies observed at different stages of their evolution rather than from a wide range of their intrinsic properties (e.g. greatly varying degrees of star forming efficiency). This result also implies that the degree of molecular gas excitation is a *consequence* of star-forming activity, rather than a *reflection of initial conditions* prior to the starburst, as often assumed. The test of the above hypothesis ultimately lies in determining the ages of starbursts in many other luminous infrared galaxies, most probably by the method of stellar population synthesis.

2. The CO-to- H_2 conversion factor X may be strongly related to the starburst phase, because the physical properties of molecular gas in an evolving starburst region changes with time as summarized before. The model X -factor shows a trend of increasing with time in the *post-SN* phase, i.e. lower values of X are associated with more highly excited gas. This is consistent with the observed results that starburst galaxies have lower values of X -factor than those of the non-starburst galaxies. The absolute numerical value for X -factor derived from our model is sensitive to the assumed initial upper mass limit of star clusters spectrum and corresponding GMC mass spectrum. In addition, the value will be affected to some degree by those factors that affect the age prediction described in Paper II.

I would like to thank my Ph.D. thesis advisor Ernie Seaquist for his guidance and support. I also thank the referee for helpful comments. This research was supported by a research grant from the Natural Sciences and Engineering Research Council of Canada to Ernie Seaquist, and a Reinhardt Graduate Student Travel Fellowship from the Department of Astronomy and Astrophysics at the University of Toronto.

REFERENCES

- Bloemen, J. B. G. M., et al. 1986, A&A, 154, 25
- Booth, R. S. & Aalto, S. 1998, in The Molecular Astrophysics of Stars and Galaxies, T. W. Hartquist & D. A. Williams (eds.), Oxford Science Publications, 437

- Boselli, A., Lequeux, J., & Gavazzi, G. 2002, *A&A*, 384, 33
- Downes, D. & Solomon, P. M. 1998, *ApJ*, 507, 615
- Dumke, M., Nieten, Ch., Thuma, G., Wielebinski, R., & Walsh, W. 2001, *A&A*, 373, 853
- Dunne, L., Eales, S., et al. 2000, *MNRAS*, 315, 115D
- Efstathiou, A., Rowan-Robinson, M., & Siebenmorgen, R. 2000, *MNRAS*, 313, 734
- Förster-Schreiber, N. M., Genzel, R., Lutz, D., & Sternberg, A. 2003, *ApJ*, 599, 193
- Gao, Y., & Solomon, P. M. 2004, *ApJS*, 152, 63
- Gao, Y., & Solomon, P. M. 2004, *ApJ*, 606, 271
- Kenney, J. D. P. & Young, J. S. 1989, *ApJ*, 344, 17
- Kennicutt, R. C., Jr. 1998, *ARA&A*, 36, 189
- Mauersberger, R. 1996, *A&A*, 305, 421
- Mauersberger, R., Henkel, C., Walsh, W., & Schulz, A. 1999, *A&A*, 341, 256
- Solomon, P. M., Downes, D., Radford, S. J. E., & Barrett, J. W. 1997, *ApJ*, 478, 144
- Strong, A. W. et al. 1988, *A&A*, 207, 1
- Thomas, H. C. et al. 2002, *MNRAS*, 329, 747
- Yao, Lihong, Seaquist, E. R., Kuno, N., & Dunne, L. 2003, *ApJ*, 588, 771
- Yao, Lihong, Bell, T., Viti, S., Yates, J. A., & Seaquist, E. R. 2006, *ApJ*, 636, 881 (Paper I)
- Yao, Lihong 2009, *Ph.D. Thesis*, University of Toronto, Canada.
- Yao, Lihong 2009, *ApJ*, 705, 766 (Paper II)
- Zhu, M., et al. 2009, *ApJ*, 706, 941